Title
SURVEY METHODS FOR NEUTRON FIELDS

Author
Moyer, B.J.

Publication Date
2011-04-04

UNIVERSITY OF CALIFORNIA

Radiation Laboratory

BERKELEY, CALIFORNIA

UCRL-1635

UNIVERSITY OF CALIFORNIA

Radiation Laboratory, Department of Physics

Contract No. W-7405-eng-48

SURVEY METHODS FOR NEUTRON FIELDS

Burton J. Moyer

January 11, 1952

Berkeley, California

SURVEY METHODS FOR NEUTRON FIELDS

Burton J. Moyer

Radiation Laboratory, Department of Physics
University of California, Berkeley, California

January 11, 1952

I. INTRODUCTION

To one whose responsibility it is to make evaluations of the degree of hazard existing in the radiation field of a nuclear accelerator or a nuclear reactor, the valid estimate of the contribution of neutrons to such a field is of considerable importance. The degree of difficulty of such a measurement depends strongly upon the information desired -- whether (1) simply the presence of "slow" and "fast" neutrons in significant numbers is in question, or (2) a measure of flux densities within known energy intervals is required, or (3) a direct estimate of the specific rate of energy absorption due to neutron-produced effects in a given medium is desired.

The importance of securing trustworthy estimates of the neutron field can be appreciated by recalling that the biological damage due to a given amount of ionization produced in biological tissue by effects due to neutrons is estimated to be several times the damage due to a similar amount of ionization produced by X-rays or gamma rays. This "relative biological effectiveness" must be evaluated by carefully controlled animal experiments. Its value appears to range from about 2.5 for slow neutrons to about 10 for fast and high energy neutrons. Of course the value obtained may also be a function of the particular biological variable under observation, and from some experiments a value as high as 20 for fast neutrons may be indicated.[1]

It is generally understood that the reason for the greater biological damage associated with neutron-produced ionization compared to that from X-rays or gamma rays lies in the matter of specific ionization. Along the tracks of recoil and secondary charged nuclear particles from neutron interactions the ionization per unit path length is typically 100 times that along the tracks of the Compton- and photo-electrons produced by X-rays and gamma rays. So even though the total energy loss per unit mass of medium were the same, these differences in local concentration of the effects will produce different degrees of damage to the organism. These same differences in specific ionization provide a basis for the selective detection of fast neutron effects in the presence of a gamma ray background.

Furthermore, the development in recent years of accelerators delivering nuclear particles with energies extending into the hundreds of Mev has introduced a few special considerations. The high-energy neutrons from such machines almost completely dominate the shielding problem, being much more penetrating than any gamma radiation.[2] Also such neutrons are capable of producing nuclear "stars" in which a large fraction of the neutron energy may be delivered into a small volume of space in the form of high-energy nuclear fragments. The quantitative, selective detection of neutrons of these energies requires instruments quite distinct from those employed in the "fast"* region.

---

* For the purposes of this discussion, the term "high energy neutrons" will mean those with kinetic energies greater than typical nuclear binding energies for a neutron. Thus, very roughly, "fast neutrons" will apply to energies above the capture resonance region and up to, say 15 Mev. "High energy" will apply from 15 or 20 Mev on up in energy.

If one is concerned simply with an evaluation of the specific energy absorption by soft biological tissue from a radiation field of any type, he may have recourse to the "tissue-equivalent" chamber technique so carefully developed by Gray, and by Failla and Rossi.[3] If prior knowledge is available concerning the relative biological effectiveness of the radiation field in question, and if it is assumed that the energy absorption in soft tissue (usually measured in the "roentgen equivalent physical" unit) multiplied by this R.B.E. will give the desired hazard index, then the use of these chambers (or of approximations thereto) is to be recommended.

The subject matter of the present article, however, assumes a desire to evaluate the various components of a radiation field, and in particular the specific neutron contributions. Methods will be described for estimating flux densities or energy absorption rates for neutrons in three energy categories: slow (i.e., thermal and near thermal), fast (0.3-15 Mev), and high energy (above 20 Mev). Whenever feasible, one desires to employ alternative methods in a given evaluation so as to provide either assurance or criticism of its validity. The discussion here submitted is certainly not exhaustive, but will involve only some of the leading ideas currently in use.

II. SLOW NEUTRON SURVEY TECHNIQUES

A. Definition of "Slow"

From the standpoint of biological effects, slow neutrons are those for which capture by nitrogen nuclei and by protons are the important phenomena in the development of absorbable energy within a biological medium.[4] This means that "slow" neutrons will here include both the thermal and capture resonance energy regions.

At these low energies the typical energy transfers by elastic collisions are neither sufficiently large to produce many ionizing particles nor to rupture many chemical bonds, and the outstanding processes by which damage may occur will be such exothermic capture events as those mentioned above. The capture by protons yields 2.2 Mev gamma radiation; and the nitrogen capture reaction is $N^{14}(n,p)C^{14}$, with 0.62 Mev energy available to the proton.

In order to selectively measure the slow neutron flux density, advantage is taken of certain unique reactions which can be easily measured even in the presence of effects due to gamma radiation and fast neutrons which may also contribute to the field. Notable among such reactions is the capture event: $B^{10}(n,\alpha)Li^7$.

B. Use of BF_3 Counters

The rate of neutron capture events in a volume V of BF_3 gas possessing N atoms of B^{10} per cm^3 is:

$$R = NV \int n(v) v\, \sigma(v) dv,$$

where n(v) is the density of neutrons per unit velocity interval at velocity v, and $\sigma(v)$ is the B^{10} capture cross section at velocity v. Since $\sigma(v)$ is nearly proportional to 1/v in the slow neutron region, it may be written as:

$$\sigma(v) = \sigma_o v_o/v,$$

where σ_o is the thermal capture cross section for B^{10} (3960 barns) and v_o is the mean thermal neutron velocity (2.2×10^5 cm/sec).

Then:

$$R = NV\,\sigma_o v_o \int n(v)dv = NV\,\sigma_o v_o\,\rho,$$

where ρ is the numerical density of slow neutrons.

Thus a BF_3 counter is, strictly speaking, sensitive to the integrated <u>numerical density</u> of neutrons within the velocity range in which the 1/v dependence is valid. If the velocity spectrum n(v) is known sufficiently well to define an average velocity $\bar{v}$, then the flux density is given by:

$$\rho\,\bar{v} = \frac{R}{NV\,\sigma_o} \cdot \frac{\bar{v}}{v_o}. \qquad (1)$$

In practice the velocity spectrum for a neutron atmosphere which has penetrated the typical shielding around a neutron source (cyclotron, etc) is sufficiently peaked at thermal energies to allow approximating $\bar{v}$ by v_o for the accuracy required in hazard evaluation. In any case, the degree to which the BF_3 is responding to neutrons above about 0.5 e v may be ascertained by enclosing the chamber with a sheet of Cd (20 or 30 mils thick), which will absorb nearly all the neutrons below this energy.

The measure of R, the rate of B^{10} capture events may be accomplished by pulse counting, the volume V being the sensitive volume of a proportional counter or of an ionization chamber. If the dimensions of the volume are large compared to the range of the alpha particle and of the recoil Li^7 nucleus, the wall effects are small, and the sensitive volume is easily estimated.[5]

The foregoing has assumed that slow neutron absorption by the counter walls is negligible. Whether or not this is true depends upon the material and thickness of the walls, and such should be so chosen as to make this effect small and calculable from known slow neutron capture cross sections. In particular, glass walls containing boron (such as pyrex glass) are to be avoided. Important aspects of preparing good BF_3 proportional counters and pulse chambers have been discussed by Fowler and Tunnicliffe.[6]

C. BF_3 Ionization Current Method

Because of the difficulty of rendering pulse amplifiers and recorders easily portable it is often convenient to make use of electrometer circuits to measure R by providing a reading of the ionization current collected out of a volume V. Since each capture event releases 2.34 Mev as kinetic energy of the alpha and Li^7 particles, and since this energy is lost by ionization and excitation with a quota of about 30 e v per ion pair, the ionization current contribution due to neutrons will be (at saturation):

$$I = (1.6 \times 10^{-19})\left(\frac{2.34 \times 10^6}{30}\right) VR\left(1 - \frac{1}{5}\,\frac{\Delta V}{V}\right) \text{ amperes,} \qquad (2)$$

where ΔV is the volume reduction accomplished by moving the chamber walls inward by a distance equal to the range of the alphas in the BF_3 gas. For BF_3 at atmospheric pressure this range is about 0.3 cm.

The volume correction factor $(1 - 1/5\ \Delta V/V)$ approximately accounts for the fact that capture events occurring near the walls may not contribute their full quota of ionization to the gas. The value of R from (2) may be used in (1) to evaluate the flux density, if one has a means of subtracting the portion of the ionization current which is contributed by gamma and other components of the field.

A particularly simple type of survey instrument consists of a pair of ionization chambers, each of about 3 liters volume, having one filled with pure, dry BF_3 to a pressure of about one-half atmosphere, and the other filled to such a pressure of Argon or CO_2 as to give an ionization current identical to that from the BF_3 chamber when both are exposed to the same intensity of Radium gamma radiation. These chambers are then arranged so that the difference current which exists in a combination slow neutron and gamma field, by virtue of the alpha reaction in the BF_3, is fed into an electrometer with a sensitivity of about 10^{-12} ampere.

With a stable, bridge-type electrometer circuit, and a BF_3 gas filling enriched isotopically in B^{10} to 96%, flux densities in the range from 10 to more than 10^4 slow neutrons/cm^2 sec are readily measurable. This is the range of interest in a region where the evaluation of safe working conditions is sought, such as the area immediately outside the shielding of an accelerator, or near an experimental facility at a reactor. In Figure 1 is shown a schematic diagram of the circuit used in a portable instrument of this type, and a photograph showing its form. It is to be noted that the chamber walls are not at ground potential, so a light-weight dural carrying case encloses them. The chambers are of brass, as thin as is compatible with their evacuation,

D. Foil Activation Methods

Usually survey work demands on-the-spot evaluations, so that direct-reading instruments involving the preceding methods are dictated. However, there are occasionally met situations where accessibility problems, or physical dimensions, require the use of the foil activation method. The ideas and techniques have been sufficiently described elsewhere.[7,8]

Of course, in order to accomplish absolute measurements of flux densities, knowledge is required of the activation cross section of the foils and of the absolute efficiency of the counting method. The latter will involve geometry, window absorption, and foil self-absorption studies. Because of these problems it is best to employ the foils simply for comparison of neutron flux densities, and if a region of known flux is available it may serve as a reference standard.

The simplest way to achieve a region of known flux density is to place a Ra-Be neutron source of determined source strength in a water tank of such dimensions that at least 30 cm of water exist in any direction from the source. A properly made Ra-Be source will yield 1.5×10^7 neutrons/sec per curie of Ra. At any distance, r, from the source which is emitting Q neutrons/sec, the thermal neutron flux density is

$$\rho v_o = Q \times f(r), \qquad (3)$$

where f(r) is the fractional number of neutrons emitted by the source which cross 1 cm^2 as thermal neutrons at distance r.

Curves of f(r) have been prepared by various experimenters.[9,10] In reference 9 the values of f(r) are usable as given. From reference 10 one must construct his curve of f(r) by dividing each datum point by r^2, and then normalizing the curve so that

$$4\pi\sigma_H N_H \int_0^\infty f(r) r^2 dr = 1;$$

where σ_H and N_H are the thermal capture cross section for hydrogen, and the number of hydrogen atoms per cm^3, respectively. This normalization is simply a statement of the fact that all neutrons emitted by the source are absorbed by hydrogen capture. The value of σ_H is 0.31 barns. In Figure 2 is displayed such a curve calculated from the data of Rush in reference 10. A certain amount of guess-work is involved in extrapolating the curve to $r = 0$.

The element most used in foil work is Indium, and the selection of thermal neutron activation from that produced by both thermal and resonance capture is accomplished by measuring activation of the foils both with and without Cadmium enclosure. The corrections due to Cd absorption of In resonance neutrons, and due to local depression of neutron flux density by the detecting foils, are discussed in reference 7. These can be made small by proper design of the experiment.

Typically, the absolute counting efficiency for thin Indium foils can be made such that a thermal neutron flux density is related to foil activity by:

$$\rho v_o = C(A - 1.07A_{Cd}), \qquad (4)$$

where C is a factor near 0.1, and A and A_{Cd} are the initial, saturated counting rates for the foils (in C/M) exposed uncovered and covered with Cd, respectively.

In summary, and for example, if one needs knowledge of the thermal neutron flux density which would exist within biological tissue located in a given neutron field, he may imbed foil detectors in a tissue-equivalent medium (water does quite well in this case) of proper size and determine the foil activation, with and without Cd envelope (.020" thick Cd is sufficient). This activation is then compared with that obtained in a water tank with known flux given by equation 3. Or, if counting efficiency is accurately calculated, so that the C in equation 4 is known, this latter formula may be used.

III. EVALUATION OF FAST NEUTRON FIELDS

A. Characteristics of "Fast" Region

In keeping with a previous definition, the concern of the present section is with neutrons extending in energy from a few tenths Mev to 15 or 20 Mev. Within this region the predominant process by which energy is delivered to a biological medium is the recoil of protons from collisions of the neutrons with hydrogen. That this is true may be readily ascertained by reference to the values and behavior of the n-p cross section and of the collision cross sections for C, O, and N in this energy region, bearing in mind the important fact that in collision with hydrogen the neutron imparts on the average half of its energy to the recoil proton, whereas in collisions with C and O nuclei the neutron loses typically only 0.14 and 0.11 of its energy, respectively.

It is obvious then that most fast neutron measurements are made by taking advantage of the simple and known characteristics of the n-p collision. Within this energy region the kinematics are those of a simple elastic billiard ball collision, i.e. there is spherical symmetry in the center-of-mass system. In Figure 3 are displayed the values of σ_{np} versus neutron energy, and the range of a recoil proton in CH_2 vs. its energy. Also shown, because of its subsequent use, is a plot of $\sigma_{np} \times R_p$.

The damage delivered to a biological medium will depend fundamentally upon the product of σ_{np} and neutron energy, since in this energy region essentially all recoil protons remain within the medium and deliver all their energy thereto. Because of the manner in which σ_{np} decreases with neutron energy, the product $E\sigma_{np}$ is nearly constant over the "fast" region. The R.B.E. of the neutrons in this region does not have pronounced dependence upon energy.

Of the survey methods described below, each has its own restricted field of validity. No one technique answers all questions about fast neutron radiation. Consequently it is necessary to give careful attention to the restrictions placed upon the conditions in energy, direction, etc. for which a given method is validly interpretable.

B. Monitoring with Nuclear Track Film

Since the tracks of recoil protons in photographic emulsion are identifiable upon development, it is possible in principle, if the hydrogen content of the emulsion is known, to evaluate an integrated neutron exposure by counting the number and lengths of such tracks per unit volume of emulsion. The careful work of Cheka[11] on this technique for the fast neutrons associated with a pile has been reported and applied in some situations.

The method suffers from the paucity of tracks from exposures within the "permissible" range, there being only about one track per two or three microscopic fields of view for a week's tolerance exposure (.03 rep of fast neutrons). Thus the measurement of typical personnel exposures is tedious and fraught with large statistical errors. In addition there are the important problems of control of water content of the emulsion, of processing, and of the effects of fading of the latent image, all of which are discussed in reference 11.

C. Energy-Insensitive Counter, Substitution Method

A counter which detects neutrons, all essentially from a given direction, with an efficiency which is quite independent of energy up to 5 to 10 Mev has been developed and described by Hanson and McKibben[12]. Since biological damage is not strongly dependent upon fast neutron energy, this type of instrument is frequently useful providing the neutrons are nearly unidirectional and within the proper energy limits.

When knowledge is desired about the fast neutron flux directly from an accelerator target, or from an aperture in shielding, this type of detector (so-called "long counter") is aimed at the source and the counting rate observed. Subsequently the production of neutrons is stopped, and a Ra-Be or Po-Be source of known strength is substituted in or near the target position while a new counting rate is observed. Because of the energy insensitivity of the long counter, these rates directly compare the fast neutron flux densities in the two cases. A known Ra-Be source placed at a known distance on the extended axis of the counter allows an approximately absolute calibration to be made, if precautions about back-scattering are observed.

D. Balanced Chamber Method

In a manner similar to that used for slow neutrons (Section II-C) a difference current technique may be employed for fast neutrons. One chamber contains argon, and is relatively insensitive to the neutrons; the other contains methane, and develops a considerable ionization current from hydrogen recoils. Pressures are adjusted to give equal sensitivities for radium gamma fields. A useful analysis of this method is given by Gamertsfelder.[13]

The method has no directional requirements, but the absolute calibration of the neutron response is difficult. Since for even a few Mev energy the proton ranges are comparable to chamber dimensions, the wall effects are not easy to evaluate. Unless very high pressures are employed, the sensitivity decreases pronouncedly with neutron energy above 2 or 3 Mev, and a knowledge of the neutron energy spectrum is essential to an evaluation of exposure rate.

In experience with this type of instrument in the radiation field outside a cyclotron shield it has been found that the contribution of ionization current by the neutron effects is small compared to that from gamma effects, and is thus difficult to evaluate well. Also the absolute magnitude of the difference current is undesirably small unless pressures of a few atmospheres are employed which introduce inconvenience in a portable instrument.

E. Attempts to Employ the Bragg-Gray Principle[14]

Reference was made in the Section I to the "tissue-equivalent" ionization chambers of Rossi and Failla, and it was there pointed out that it is not possible with them alone to distinguish neutron-produced ionization from gamma-produced ionization, and that this distinction is important because of the different R.B.E.

Hurst[15] describes the means of rejecting the secondary electron ionization by the expedient of biased proportional counting in an approximately tissue-equivalent gas counter with hydrogenous walls. Actually the gas was CH_4, and the wall material $(CH_2)_n$. Ideally the gas amplification and electronic amplification of the pulses magnify the energy loss events due to the recoil particles in the gas, and the output pulses are integrated into a current which is then proportional to the rate of energy absorption in the gas. This in turn is related to energy absorption in the wall material ("tissue") by knowledge of counter volume, and the stopping power ratio and density ratio for the counter gas and wall material.

By adjusting the bias level properly, only those pulses which are above the maximum size produced by secondary electrons will be admitted to the pulse-integrating circuit. Thus only recoil proton pulses will be recorded, and unavoidably the smaller of these will be rejected. If amplifications are uniform and known, a calculation of energy absorption rate in terms of integrated pulse current may be simply made.

Consider then such a proportional counter, with hydrogenous walls and gas of essentially the same hydrogen content per gram, and of reasonably identical stopping powers (on a gm/cm^2 basis). The wall thickness is to be at least as great as the range of the most energetic recoil protons, but not thick enough to produce appreciable attenuation of the fast neutrons, and the overall dimensions and location of the chamber relative to the neutron source are to be such that the neutron field intensity throughout is constant. Under such conditions the mean density of ionization events is uniform throughout the counter volume, and is, in fact, the same as if the solid walls were replaced by counter gas extending in any direction at least as fas as the most energetic protons from that direction would travel (assuming also that the uniformity of field extended to such distances).

Consequently the ionization events within the chamber are representative of those within the gas without solid walls, and the energy absorption per unit volume is simply proportional to density. The energy absorption *per gram* is thus independent of density and will be equal to the absorption per gram in the chemically similar wall material. So if the energy absorption rate in ergs/gm sec for the wall material is W, the metered output pulse current in amperes is:

$$I = (3.1 \times 10^{-9})\, A\, V\, \rho_g\, W,$$

where 0.51×10^{-10} ergs/ion pair has been assumed, and where A is the overall charge amplification of an ionization event due to both gas and electronic amplification, V is the counting volume, and ρ_g is the gas density.

Thus, if a tolerable fast neutron exposure rate were stated as 0.03 rep/week, to be accumulated on a 48 hr/week basis, the energy absorption rate on the basis of 95 ergs/gm per rep would be:

$$W = 1.65 \times 10^{-5} \text{ ergs/gm sec;}$$

and the output current per cm^3 of counting volume, with methane pressure of one atmosphere would be:

$$I_1 = (3.4 \times 10^{-17})A \text{ amperes.}$$

A volume of 50 cm^3 and a total amplification of 10^4 would produce a current readily measurable by simple electrometer circuits. The counting volume must be kept rather small so that the compton electron path lengths, whose pulses must determine the minimum pulse size accepted, will not encroach too much on the pulse distribution from recoil protons.

It is a prime requirement that the gas amplification be known and uniform throughout the counting volume. Special counter end configurations and guard ring systems have been devised[16] for approximating this condition. The necessity of biasing out the electron-produced pulses causes a failure to measure the contribution of energy dissipation from protons producing pulses below this level, and the seriousness of this will depend upon the neutron spectrum.

Possibly it is worthwhile to point out that if the neutron spectrum is sufficiently well known to allow an estimation of a mean value for $\sigma_{np}(E)\,E$, the actual neutron flux may be estimated. This follows from the fact that the energy absorbed due to hydrogen collisions per gram of the gas is given by:

$$W_H = \frac{N_H}{\rho_g} \int_0^{E_{max}} \phi(E)\, \sigma_{np}(E)\, (E/2)\, dE \quad \text{ergs/gm sec;}$$

This assumes that a neutron makes only one collision, at most, in the counter gas or wall, which is a good assumption for fast neutrons and counters of typical size.

The symbols employed denote:

N_H = hydrogen atoms/cm^3 of gas,

ρ_g = gas density in gm/cm^3,

$\phi(E)$ = flux density per unit range of energy, in neutrons/cm^2 sec erg,

$\sigma_{np}(E)$ = total n-p cross section for neutron energy E.

The average energy transfer in the n-p collision is considered to be E/2.

The corresponding expression for the collisions with carbon nuclei is:

$$W_c = \frac{N_c}{\rho_g} \int_0^{E_{max}} \phi(E) \ \sigma_c(E) \left(\frac{2M}{(M \quad 1)^2} \quad E \right) dE,$$

where M = 12 is the relative mass of the carbon nucleus.

Plotted in Figure 4 are curves of $\sigma_{np}(E)$, $\sigma_c(E)$, and of the quantity:

$U(E) = N_H \sigma_{np}(E)\ (E/2) + N_c\ \sigma_c(E) \left(\frac{2M}{(M \quad 1)^2} E \right)$, for a CH_2 medium. This last quantity is proportional to energy absorption rate per unit neutron flux density at the various energies.

If the spectrum is known with enough confidence to estimate average values $\overline{\sigma_{np} E}$ and $\overline{\sigma_c E}$, the total energy absorption is:

$$W_H + W_c = \frac{1}{\rho_g} \left\{ \frac{N_H}{2} \ \overline{\sigma_{np} E} + \frac{2MN_c}{(M \quad 1)^2} \ \overline{\sigma_c E} \right\} \int_0^{E_{max}} \phi(E) dE.$$

The integral is of course the total neutron flux density. The bias to eliminate electron pulses prevents an actual value of zero for the lower limit.

F. Directional Count-Rate Meter for "Tissue Dose"

By judicious construction of the end-wall of a cylindrical proportional counter Hurst and Ritchie[17] have succeeded in producing a counting-rate response, for a uni-directional neutron flux, whose energy dependence closely approximates the function U(E) for a tissue-equivalent medium. It is very similar to the U(E) plotted in Figure 4 for CH_2. Tests in mono-energetic, directional neutron fluxes have substantiated the calculations for their counter, but it must be noted that it is valid only for a uni-directional flux normal to the special end wall. The "tissue dose" it measures is that due to the first collisions of the incident neutrons; thus it applies to a region of the order of one mean free path in depth.

G. Measurement of Fast Neutron Energy Flux Density

Evaluation of neutron flux densities for monoenergetic neutrons is relatively straight-forward[16], but in survey work for radiation protection purposes such spectra do not typically exist. It is still quite possible, however, to measure the energy flow per cm^2 per sec carried by the fast neutrons. Then if the spectrum is known sufficiently well to estimate an effective mean energy, the numerical integral flux density may be approximated. This technique has been developed by Mather, Moyer, Redmond, and Thompson[18] at the University of California Radiation Laboratory.

The analysis of the energy-flux counter proceeds as follows in five steps:

1. Consider a plane sheet of hydrogenous material of thickness s immersed in an isotropic flux of neutrons of energy E. From any volume element recoil protons will originate with equal probability in any direction, and with equal

probability in energy up to the maximum possible value of E. The number of protons produced in dV at depth x which will emerge with sufficient residual range to be detected may be shown[18] to be: (See Figure 5)

$$dF(X,E) = \frac{1}{2}\,\phi(E)\;\sigma_{np}(E)N_H dV \int_{\epsilon_x}^{1} \left(1 - \frac{X}{R(\epsilon) - r}\right) d\epsilon \,; \qquad (5)$$

where: $\epsilon = \frac{Ep}{E}$ = fractional energy delivered to a recoil proton,

ϵ_x = minimum fractional energy for emergence from depth x,

$R(\epsilon)$ = range in the hydrogenous material of a proton with fractional energy ϵ,

and r = residual range required upon emergence to allow detection.

(The other symbols have the same meaning as in Section E, above).

2. If now $R(\epsilon)$ is approximated by $R(E)\ \epsilon^{3/2}$, where R(E) is the proton range for $\epsilon = 1$; and if, to begin with, the required residual range r is set equal to zero, expression (5) may be integrated to yield:

$$dF(X,E) = \frac{1}{2}\,\phi(E)\;\sigma_{np}(E)\left\{1 + \frac{2x}{R(E)} - 3\left(\frac{x}{R(E)}\right)^{2/3}\right\} N_H dV. \qquad (6)$$

This last approximation of $r = 0$ is <u>not</u> employed in more precise calculations[18] which space does not allow here.

3. The contributions from all depths x are now to be summed. Denote volume element dV by Adx, where A is a plane area parallel to the surface. Then by integration over x the results may be obtained for the two cases (a) $s \geq R(E)$, and (b) $s < R(E)$.

(a) $S \geq R(E)$

$$F(E) = \frac{1}{2}\,\phi(E)\,\sigma_{np}(E)\,N_H\,A \int_0^{R(E)} \left\{ 1 + \frac{2x}{R(E)} - 3\left(\frac{x}{R(E)}\right)^{2/3} \right\} dx$$

$$= \frac{1}{10}\,N_H A\,\phi(E)\,\sigma_{np}(E)\,R(E). \qquad (7)$$

(b) $S < R(E)$

$$F(E,S) = \frac{1}{2}\,\phi\,\sigma\,N_H\,A \int_0^{S} \left\{ 1 + \frac{2X}{R} - 3\left(\frac{X}{R}\right)^{2/3} \right\} dX$$

$$= \frac{1}{2}\,N_H\,A\,\phi(E)\,\sigma_{np}(E)\,R(E) \left\{ \frac{S}{R} + \frac{S^2}{R^2} - \frac{9}{5}\left(\frac{S}{R}\right)^{5/3} \right\}. \qquad (8)$$

Expressions (7) or (8) will give the number of protons emerging each second from one face of the sheet, having been produced within the parallelepiped volume AS by neutrons of energy E.

4. The total number of protons emerging per second is to be obtained by integrating over the energy spectrum. This integration is divided into two parts: (a) Energy interval from $E = 0$ to $E = E_s$, where E_s is the energy required to give range S in the sheet material, and (b) Energy interval from E_s to infinity, or to E_{max} for the spectrum of the neutrons. Thus if every proton which emerges can be counted, the counting rate arising from area A will be:

$$C = \int_0^{E_s} F(E)\,dE + \int_{E_s}^{E_{max}} F(E,S)\,dE; \qquad (9)$$

where F(E) and F(E,S) are expressions (7) and (8), respectively.

In many instances $S > R(E_{max})$, so that only the first term of (9) is involved. (For example, the range of a 15 Mev proton in polyethylene is only 0.24 cm or 3/32 inch, which would be quite reasonable a wall thickness). Advantage is now taken of the fact evident from Figure 3, that over a wide range of energies in this region the product $\sigma_{np}(E)\ R(E)$ is very nearly proportional to E. From less than 0.1 Mev up to 20 Mev the approximation:

$$\sigma R \cong (1.0 \times 10^{-26})\ E, \tag{10}$$

with E expressed in Mev, and the product σR (in cm^3) is nowhere in error by more than 15%.

Thus for a sheet whose thickness is greater than $R(E_{max})$, so that only the first integral of (9) is required, C becomes, in view of (7) and (10):

$$C \cong (1.0 \times 10^{-27})\ N_H\ A \int_0^{E_{max}} \phi(E)\ EdE, \text{ cts/sec.} \tag{11}$$

The integral appearing here gives the total energy flux density carried by fast neutrons. Corrections to this somewhat oversimplified discussion are mentioned in the next step.

5. The sheet of CH_2 is now bent into a cylinder whose radius is large compared with S, and is very lightly graphited with aquadag to provide conduction. It is then made to serve as the cathode of a proportional counter filled with argon plus a small percentage of CO_2.

The refinements to the foregoing calculation involve the following items:

(a) Treatment of the problem with r not zero, i.e., with a specified residual range required for detection.

(b) Effects of Argon and Carbon recoils.

(c) Geometrical effect of bending the flat sheet into a cylinder.

(d) Inclusion of neutron energies for which $R(E) > S$, i.e., the use of both terms of Equation (9).

The results of such a calculation are displayed for various CH_2 sheet thicknesses in Figure 6, in which the ordinate is efficiency in counts/unit area per unit flux density of neutrons in unit energy interval at E. It is evident that below 1 Mev the requirement of a residual range which will provide as much as a 0.2 Mev energy loss in the counter gas reduces the efficiency markedly below proportionality to neutron energy; however, 0.2 Mev is possibly a more stringent requirement than is necessary if proper counter design keeps electron path lengths short. Actually the curves of Figure 6 do not contain corrections (b) and (c), and the contribution of argon for a typical counter is indicated separately. Correction (c) can be estimated to be small for a typical counter diameter of 5 cm, though its effects at the higher energy end begin to be appreciable.

From Figure 6 it is seen that if the spectral region of interest lies between 0.8 Mev and nearly 20 Mev, a 1/8" wall counter has a sensitivity essentially proportional to energy, and the simple relationship of Equation (11) may be used. If values of residual proton range r smaller than 0.2 Mev equivalent are possible (see below), the lower energy limit of this proportional region is moved downward as is indicated by the ideal curve for $r \simeq 0$.

In Figures 7 and 8 are shown two distinctly different types of survey units employing the foregoing principles. The first is a polyethylene-wall proportional counter, and the second is a polyethylene spherical shell whose inner surface is coated with a phosphor. Recoil protons produce scintillations which are viewed with an end-window photomultiplier tube through a suitable aperture. In each case the primary pulses, after amplification and discrimination, trigger a one-shot multivibrator whose output is integrated into a counting-rate reading.

The spherical scintillation counter has certain advantages. The fast neutron radiation outside the shielding of an accelerator is not completely isotropic, and the spherical geometry removes the requirement of isotropy. (However, it should be mentioned that the requirement of isotropy for the cylindrical proportional counter is certainly not stringent, as it would be for the flat sheet.) Another advantage is the possibility that electron pulses can be more favorably rejected because of their small energy loss in the very thin layer of phosphor, thus allowing the use of a small value for r, the residual proton range for detection.

As an example, with the spherical counter shown, the discriminator was set so as to reject all counts from a radium gamma field of 30 mr/hr. The counter was then tested with a known Po-Be source in an energy flux density calculated from the Po-Be spectrum. The experimental result was:

$$1 \text{ count/sec for } 15.9 \text{ Mev/cm}^2 \text{ sec.}$$

The calculated counting sensitivity from Equation (11) was:

$$1 \text{ count/sec for } 13.9 \text{ Mev/cm}^2 \text{ sec.}$$

Corrections for inefficiencies at low energies, as indicated in Figure 6, would tend to bring the numbers closer, but agreement to better than 15% can be considered fair for survey counters. This degree of agreement has consistently been found with both the proportional counters and the scintillation counter.

IV. ESTIMATION OF HIGH ENERGY NEUTRON FLUX DENSITIES

A. Character of Neutron Field Spectra

Accelerators of nuclear particles in the hundreds of Mev region produce large numbers of neutrons extending in energy up to the primary energy of the nucleons accelerated. Because of the great penetration of such neutrons through shielding matter, and because nuclear cross sections decrease monotonically with neutron energy in this region, the neutron radiation escaping from the outer surface of a thick shield wall will consist of the equilibrium secondary neutrons accompanying the penetrating primary component. After the initial transition region, in which the soft components of the primary radiation are rapidly absorbed and the secondary neutron radiation is developed into equilibrium with the high energy components of the primary, the ensuing attenuation is controlled by the penetration of these high-energy primary components.

In consequence of this, the neutron spectrum external to a thick concrete shield should decrease monotonically from the thermal energy spectral intensity to that at higher energy. If one can then make flux measurements at thermal energies, in the "fast" region, and at high energy, he can roughly delineate the total picture. Because of the low flux of the high-energy component when its equilibrium secondary radiation is within tolerance bounds, and because of its relatively low interaction cross section with matter, this high-energy component is difficult to measure on a survey basis.

B. Nuclear Stars and Recoils

The ejection of fast charged nuclear particles from nuclei struck by high energy neutrons produce characteristic "stars" in photographic emulsion. Knowledge of the nuclear composition of the emulsion, and estimates of cross-sections for star production in various elements allow approximate flux evaluations if cross sections are not strongly energy-dependent.

As an example of such a procedure the data pertaining to a certain situation near the 184" Cyclotron will be quoted:

(a) The composite inelastic collision cross section per cubic centimeter of the emulsion was calculated from the known chemical constituents, and from the total nuclear collision cross sections at 90 Mev (assumed in this case to be an effective energy for the high energy components outside the shielding). At these energies, inelastic collision cross sections are almost exactly one-half the total cross sections. Thus:

$$\frac{1}{2} \sum \sigma_i N_i = .041 \text{ cm}^2 \text{ per cm}^3 \text{ of emulsion.}$$

(b) It was assumed that about 1/3 of this composite inelastic cross section resulted in identifiable stars.

(c) The star production rate was found to be 0.3 stars/mm^3 per hour, or .08/cm^3 sec.

(d) Thus the high-energy neutron flux density was estimated to be:

$$\phi = \frac{.08}{1/3\ (.041)} \simeq 6/\text{cm}^2 \text{ sec.}$$

C. Bismuth Fission Counter

Fission of the Bi nucleus by high-energy neutrons sets in at about 50 Mev, and appears to rise regularly in its cross section up to over 300 Mev. A design of Bi fission counting chamber by Wiegand[19] has served as a prototype for those employed in survey work.

The fission cross section of Bi under neutron bombardment has been measured to be 0.05×10^{-24} cm^2 at 84 Mev. This of course means that the efficiency of the counters is low, since the useful thickness of the Bi layers is limited by the range of the fission fragments. In fact, in order to take survey data in fields of a few high energy neutrons per cm^2 per second, it is necessary to use counting periods of the order of hours. However, the method has frequently proved useful, since little else is available as a survey meter. A rough absolute efficiency is calculable from the above cross section, the ranges of fission fragments, and from geometrical considerations on the emergence of the fragments from the Bi layer.

V. ACKNOWLEDGEMENTS

It is a pleasure to acknowledge the association with Messrs. W. E. Nolan, W. Patterson, B. W. Thompson, A. Redmond, and of Dr. R. L. Mather, in the application of several of these techniques and in the development of a few of them.

REFERENCES

1. See summary by Evans, T. C., Nucleonics 4, No. 3, 2-8 March (1949).
2. Hildebrand and Moyer, Phys. Rev. 72, 1258-1260 (1947).
3. See Vol. 2, p. 603, in "Medical Physics", O. Glasser, editor, Yearbook Publishers, Inc., Chicago, 1950.
4. Tait, J. H., Calculation of Energy Deposition in Soft Tissue by Thermal Neutrons, AERE-TR-416, October, 1949.
5. Rossi and Staub, "Ionization Chambers and Counters", Chapter 8, and Appendix 9. National Nuclear Energy Series, McGraw-Hill Book Co., New York, 1949.
6. Fowler and Tunnicliffe, Rev. Sci. Inst. 21, 734 (1950).
7. "Science and Engineering of Nuclear Power", edited by Clark Goodman, Addison Wesley Press, Inc., Cambridge, Mass., 1947, pp 210-215.
8. Tittle, C. W., Nucleonics 8, No. 6, 5-9, June 1951; and Nucleonics 9, No. 1, 60-67, July 1951.
9. Agnew, et. al., MDDC-878, Sept. 7, 1942 (Declassified Jan. 3, 1947).
10. Rush, J. H., Phys. Rev. 73, 271-3 (1948).
11. Cheka, J. S., "Neutron Monitoring by Means of Nuclear Track Film", ORNL-547, Jan. 9, 1950.
12. Hanson, A. O., and McKibben, J. L., Phys. Rev. 72, 673 (1947). See also reference 5 above.
13. Gamertsfelder, C. C., "Calculations for Use with the Fast Neutron Meter", AECD-2173, July 1948.
14. Gray, L. H., Proc. Camb. Phil. Soc. 40, 72 (1944).
15. Hurst, G. S., Ra-Det 2, No. 4, 43-47, Sept. 1949.
16. See Chapters 4 and 7 of Reference 5.
17. Hurst, G. S. and Ritchie, R. H., "A Count-Rate Method of Measuring Fast Neutron Tissue Dose", ORNL-930, Jan. 30, 1951.

18. In preparation for publication. (R. L. Mather, B. J. Moyer and B. W. Thompson).

19. Wiegand, C., Rev. Sci. Instr. 19, 790 (1948).

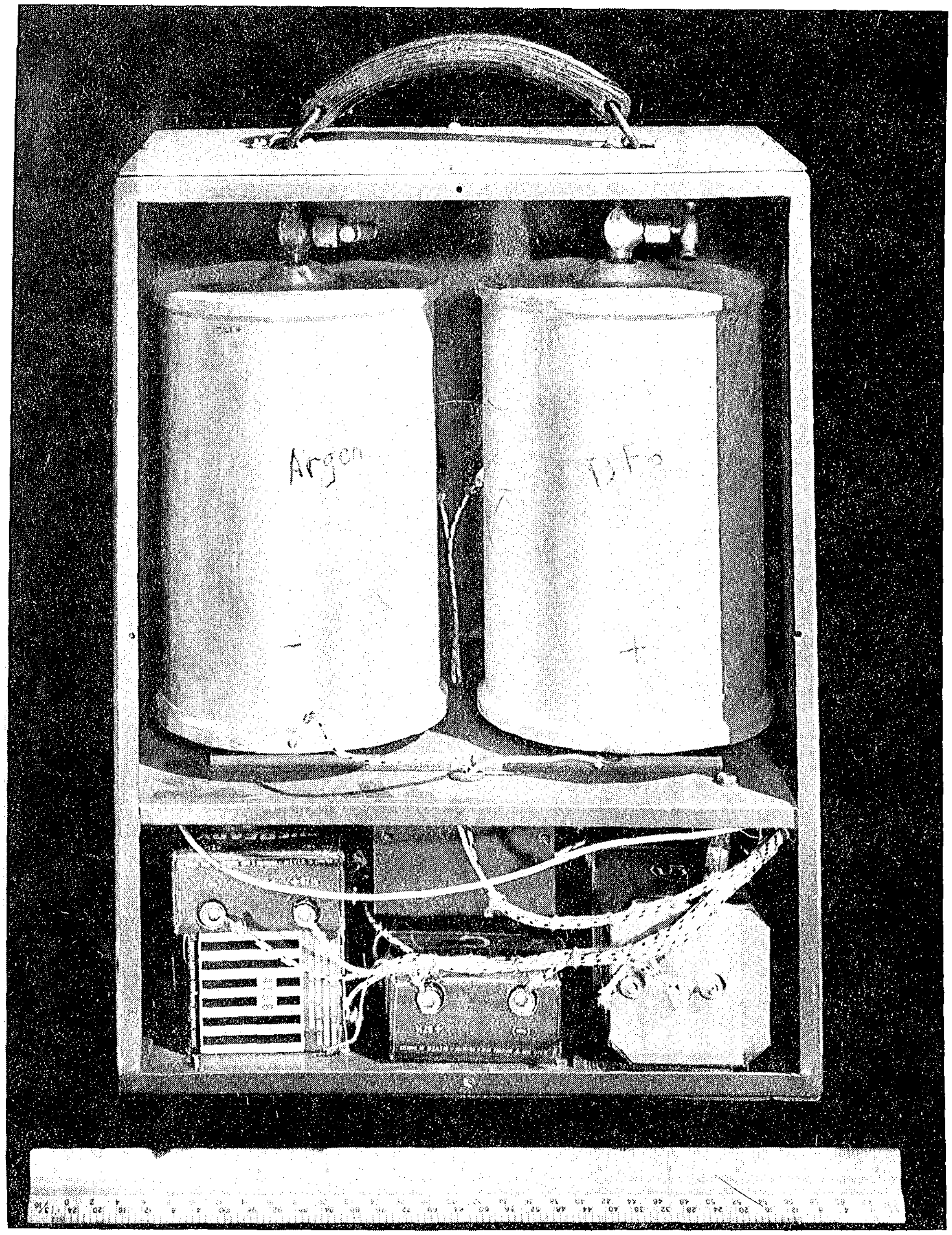

ZN 211

Fig. 1(a).

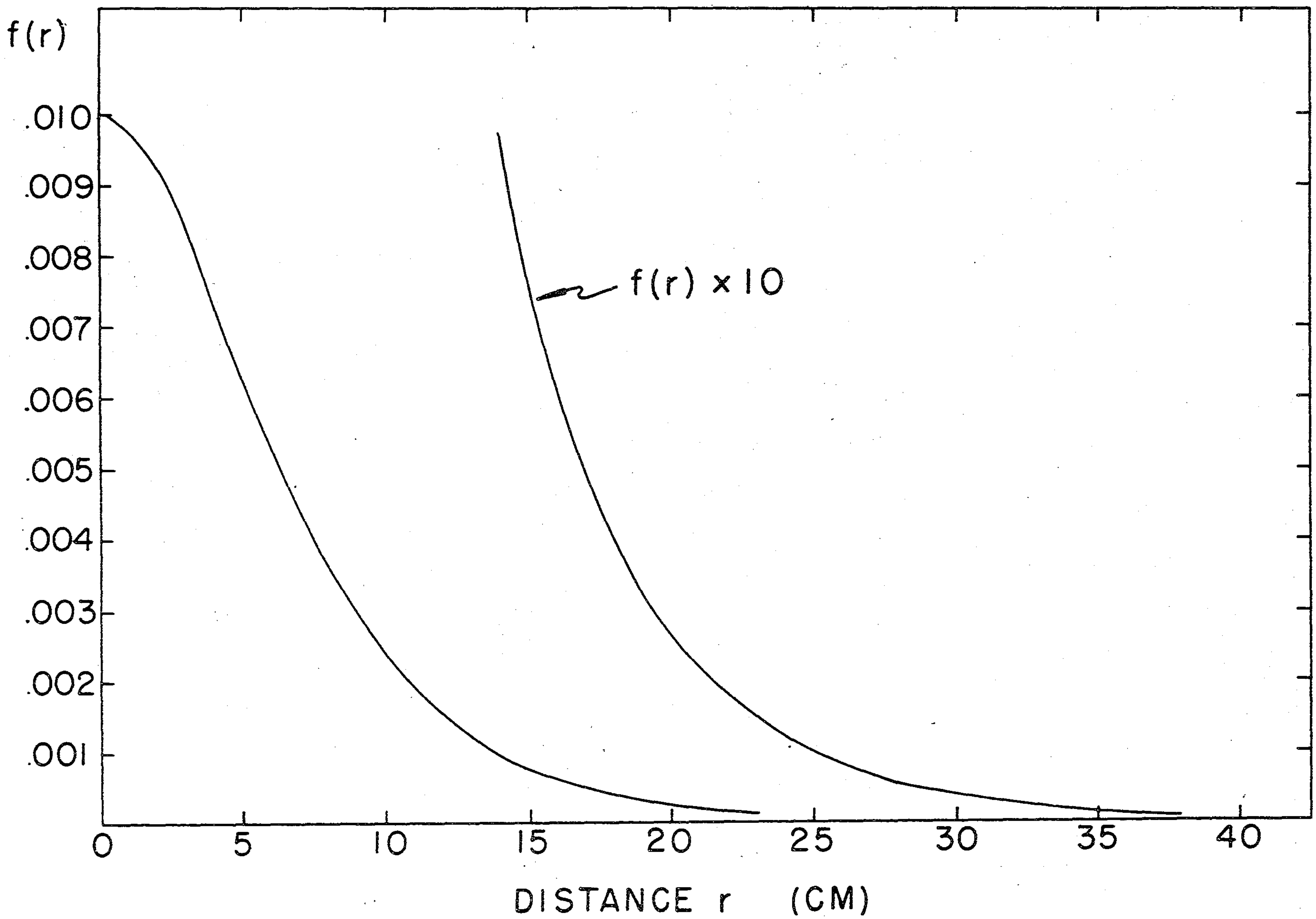
f(r)
.010
.009
.008
.007
.006
.005
.004
.003
.002
.001
f(r) x 10
0
5
10
15
20
25
30
35
40
DISTANCE r (CM)

189621

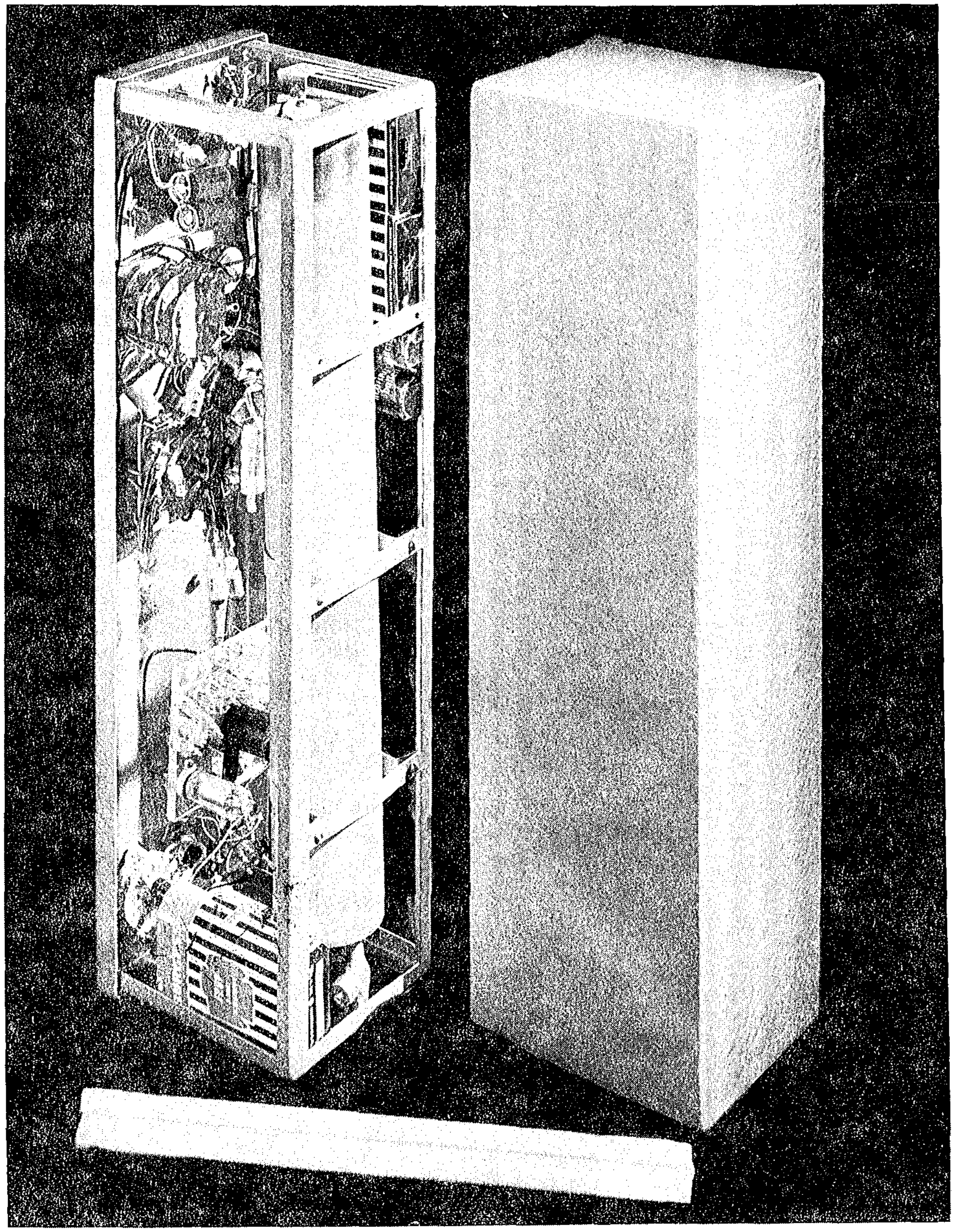

ZN 210

Fig. 7.

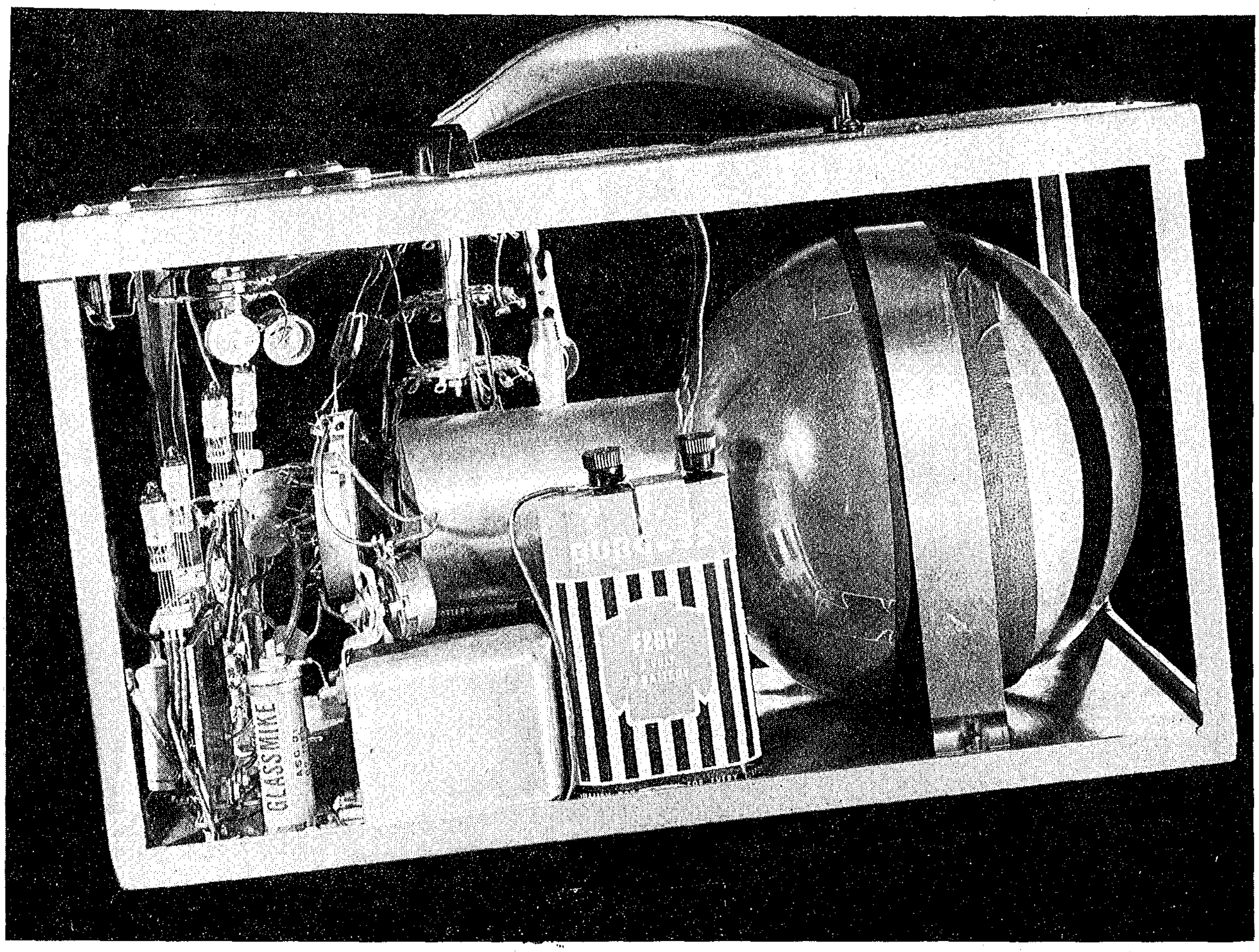

ZN 212

Fig. 8.